

Title: Some Considerations on High Power From Operating GEO600

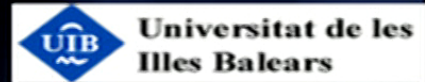
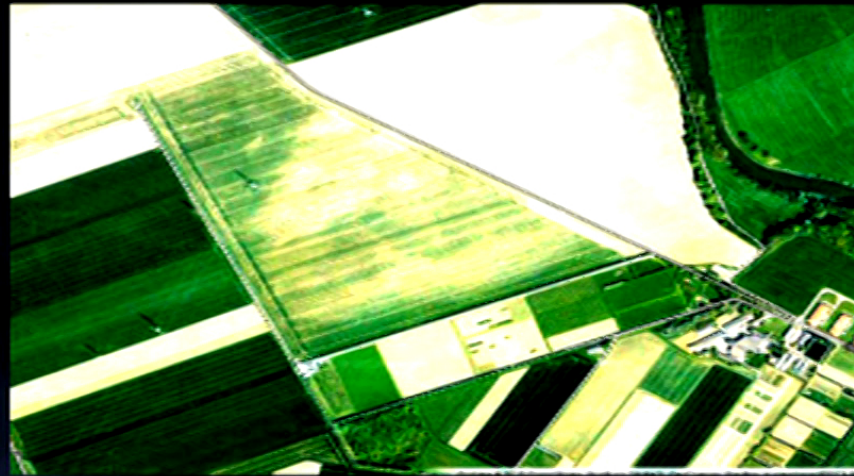
Date: Jun 13, 2018 02:00 PM

URL: <http://pirsa.org/18060059>

Abstract:



# GEO600



Hartmut Grote  
for the GEO team

Perimeter Workshop  
2018

CARDIFF  
UNIVERSITY





# Lasers



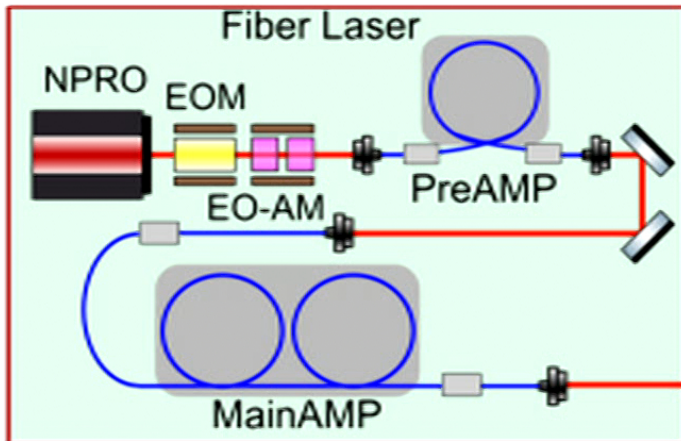
## High Power Laser for future Gravitational Wave Detectors

- no large commercial interest in high power lasers in fundamental spatial mode with low noise
- solid-state laser spatial beam profile suffers from depolarization (mode selective pumping) or spurious modes (homogeneous pumping)
- depolarization is suppressed in birefringent material (e.g. Nd:Vanadat)
- current limit of Nd:Vanadat amplifier with good spatial profile 100W
- fiber amplifiers which have shown good spatial profile and low noise performance BUT have not yet been operated reliable in GWD labs
- coherent combination with good spatial profile has been demonstrated at power level of 50W \*
- most likely path to 500W GWD laser is currently the coherent combination of two or more fiber amplifier

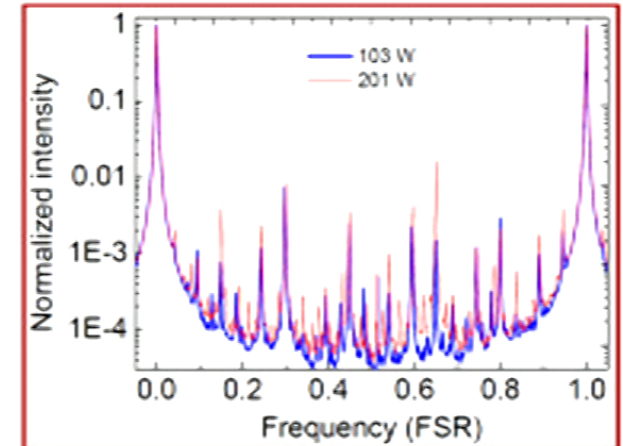
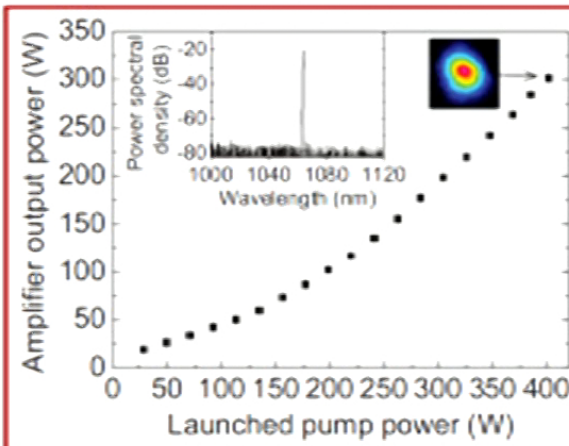
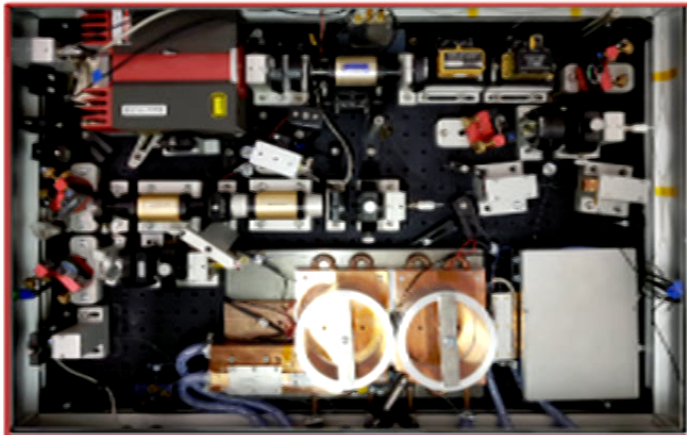




## 300W Fiber Amplifier at 1064nm



- two stage fiber amplifier with NPRO seed
- good spatial profile
- output power up to 300W
- so far no long-term reliable operation



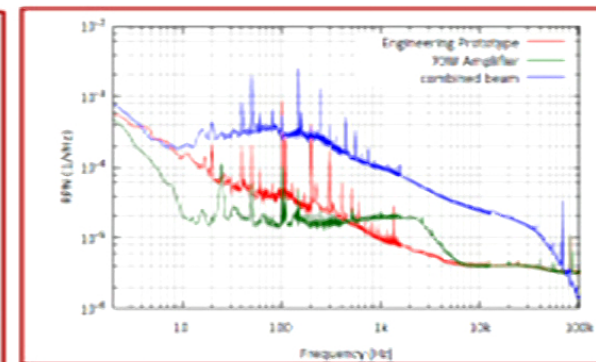
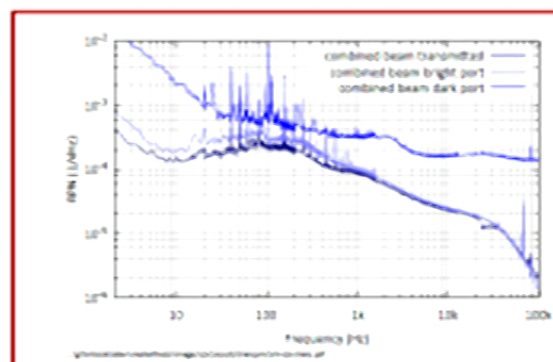
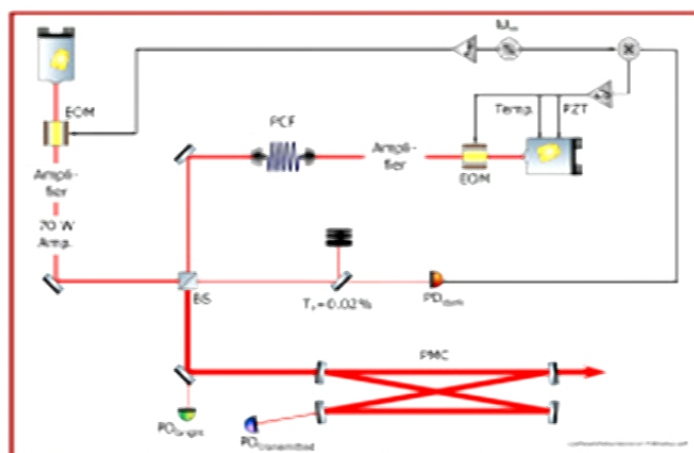
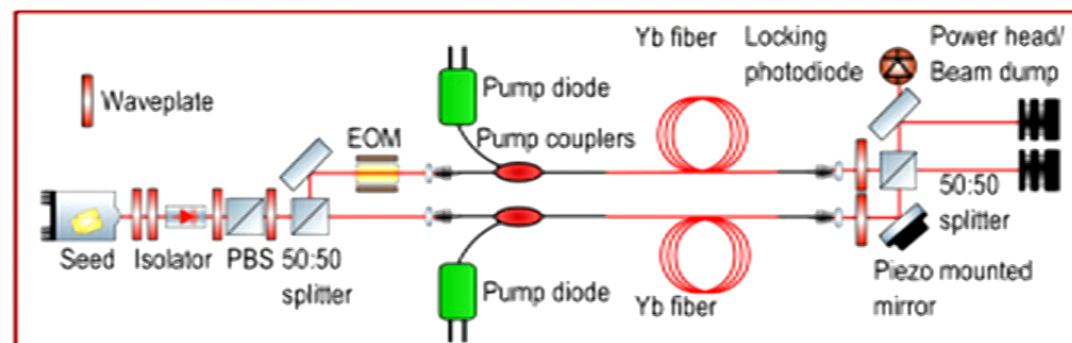
T. Theeg et al. IEEE Photon. Tech. Lett. (2012); T. Theeg et al. Opt. Express (2012)



# Coherent Beam Combination at AEI / LZH

proof of principle experiments with

- two independent 5W beams taken from 70W and 35W laser
- two identically seeded 10W fiber amplifiers
- next step: two 150W lasers
- final goal: 2x250W



H. Tuennermann et al., Opt. Express (2011)

# Power Increase (in GEO)

# Power Increase (in GEO)

- Saturations



# Power Increase (in GEO)

- Saturations
- Scattered light to local control shadow sensors

# Power Increase (in GEO)

- Saturations
- Scattered light to local control shadow sensors
- Power instabilities due to clipping and radiation pressure



# Power Increase (in GEO)

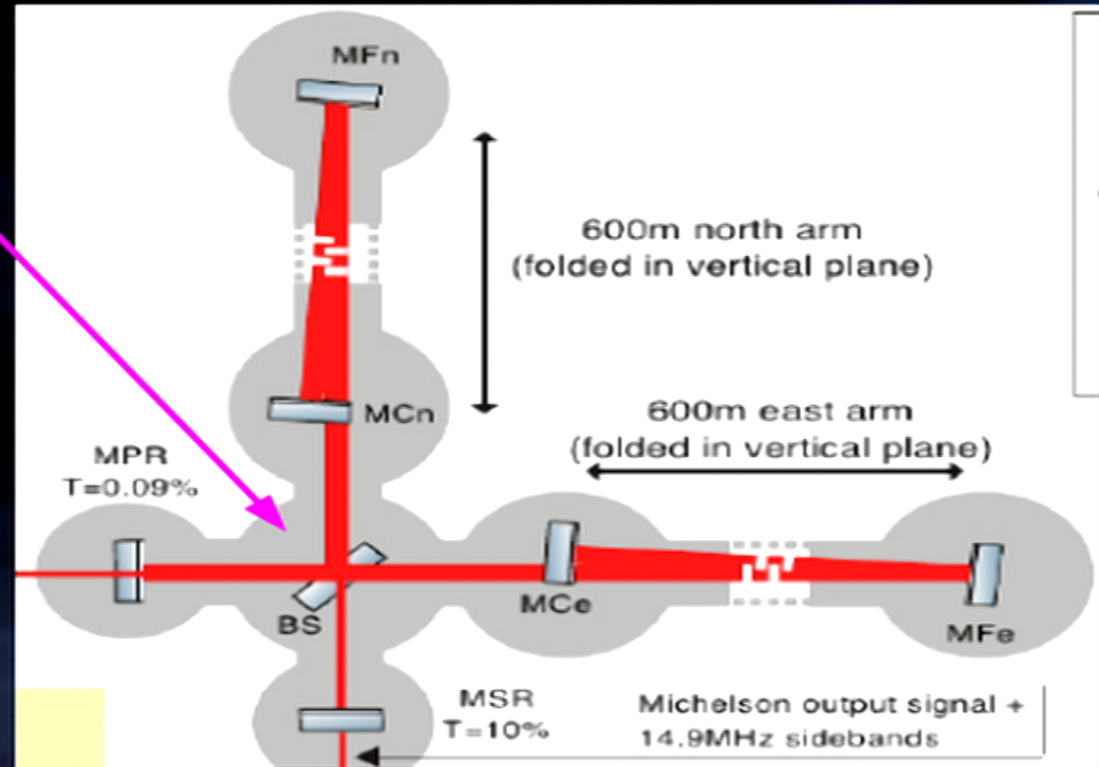
- Saturations
- Scattered light to local control shadow sensors
- Power instabilities due to clipping and radiation pressure
- Thermal Lensing (here: beamsplitter)



# Thermal compensation for the beamsplitter

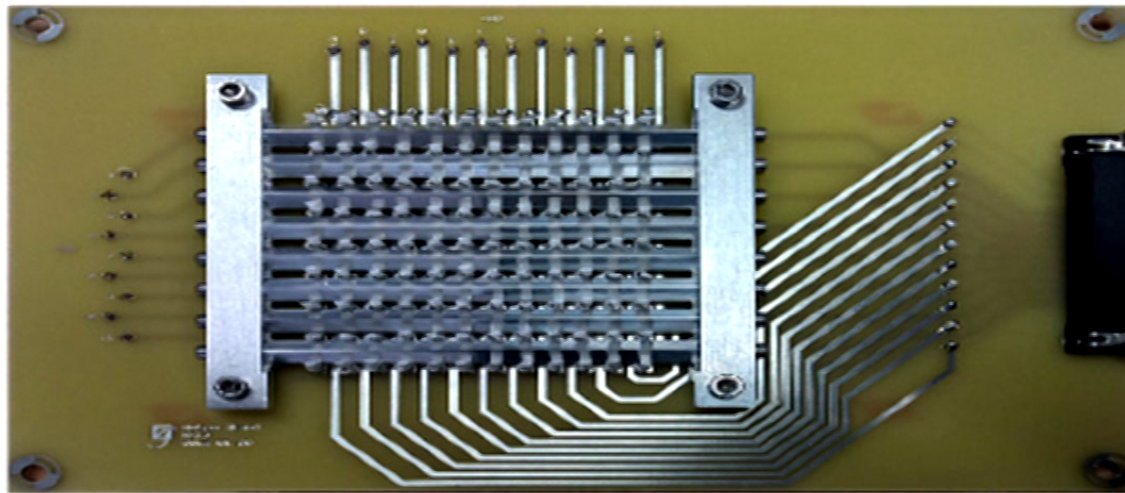
# Power – up challenges

- ~3 kW at beamsplitter (no arm cavities)
- High power causes thermal lens in one arm, degrading contrast at the output
- Consequences for stray light and control
- Use compensation plate ?

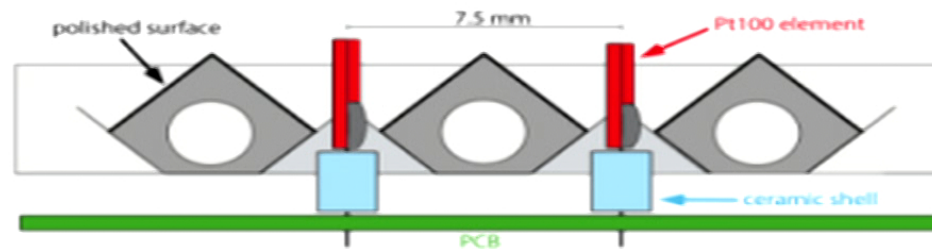




# Thermal compensation with a matrix of thermal radiation pixels



(a) Photograph of the heater array.



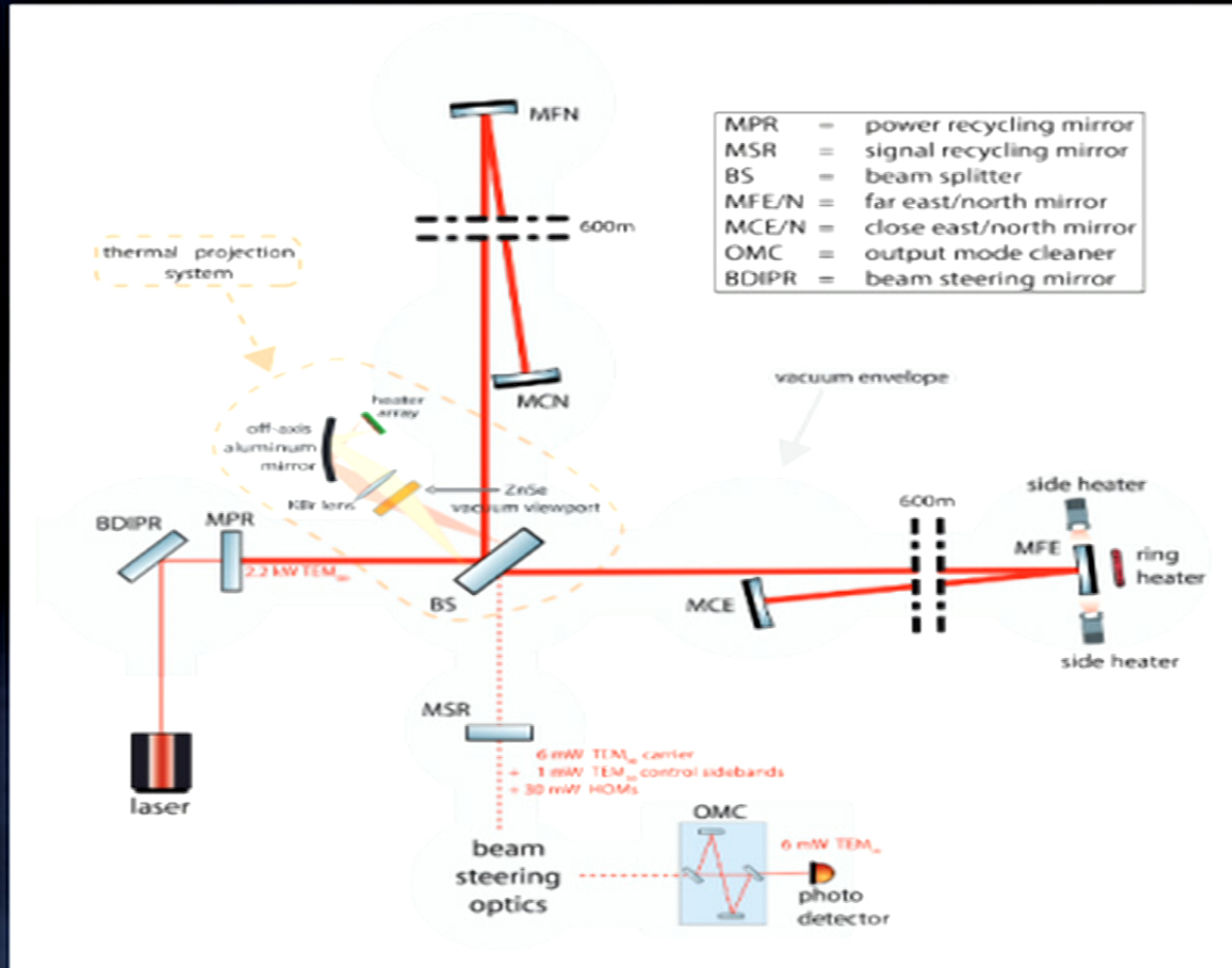
(b) Cross section of the heater array.





H. Wittel

# GEO600 / matrix heater Layout

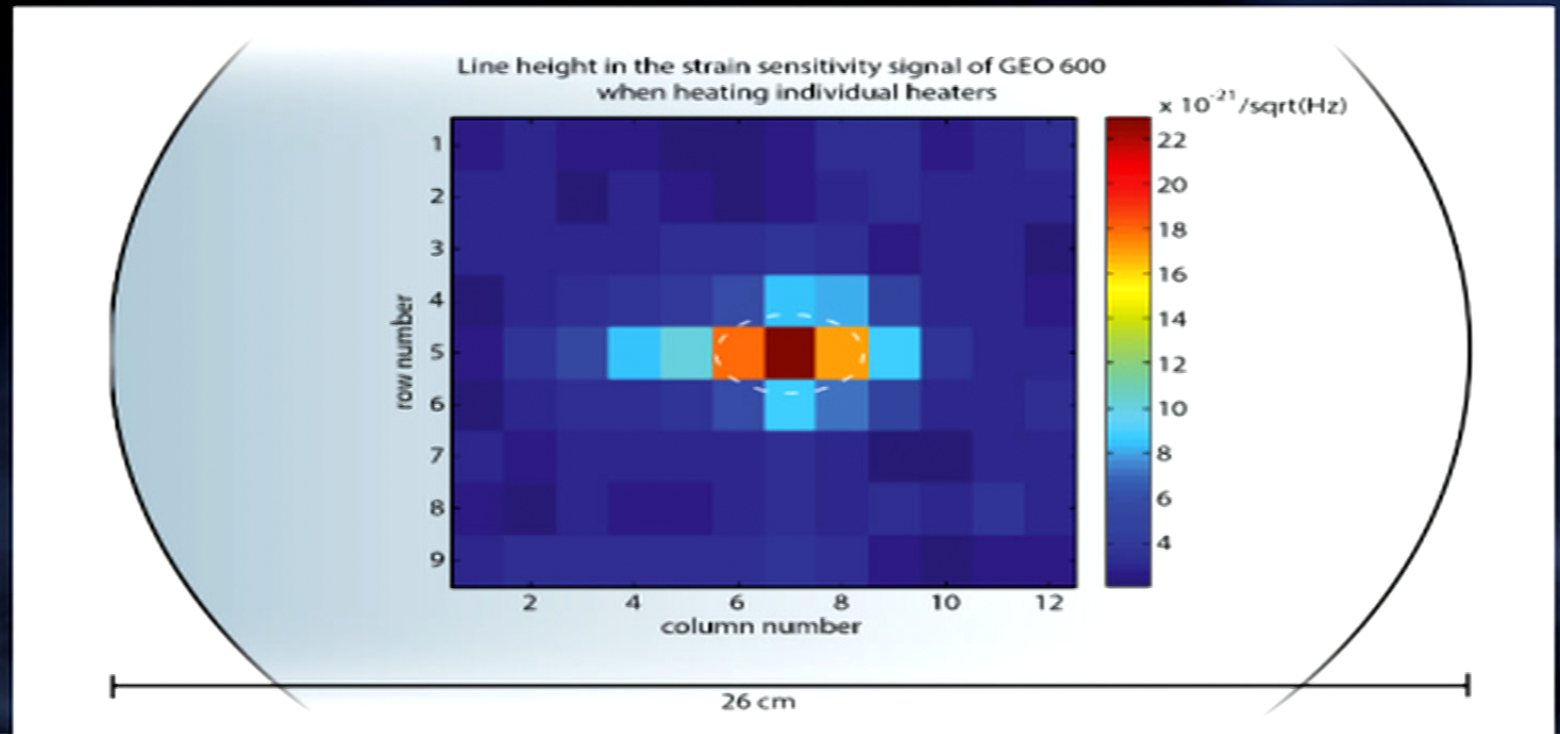


H. Wittel



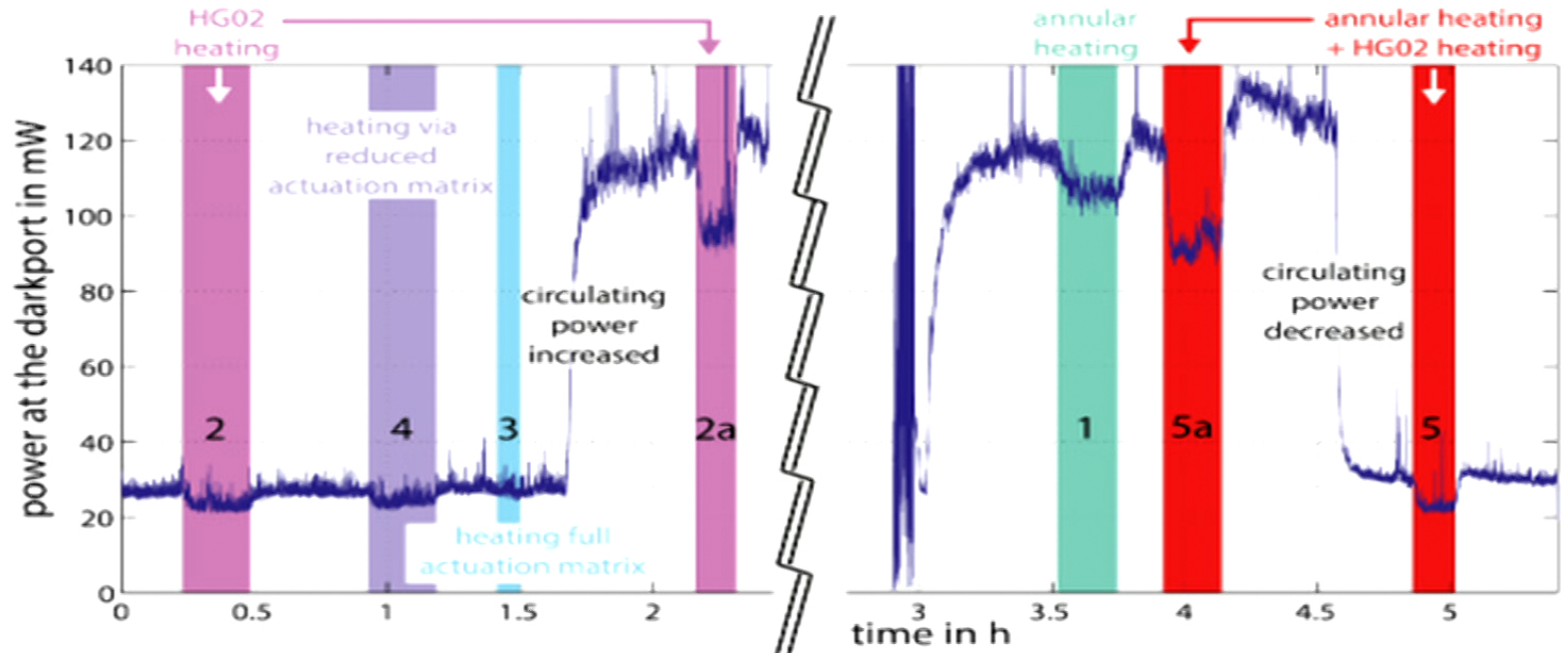
# Mapping the beam with the heater array

- Modulate each pixel and record line height in DARM
- Overlap of heater with main beam → used for alignment

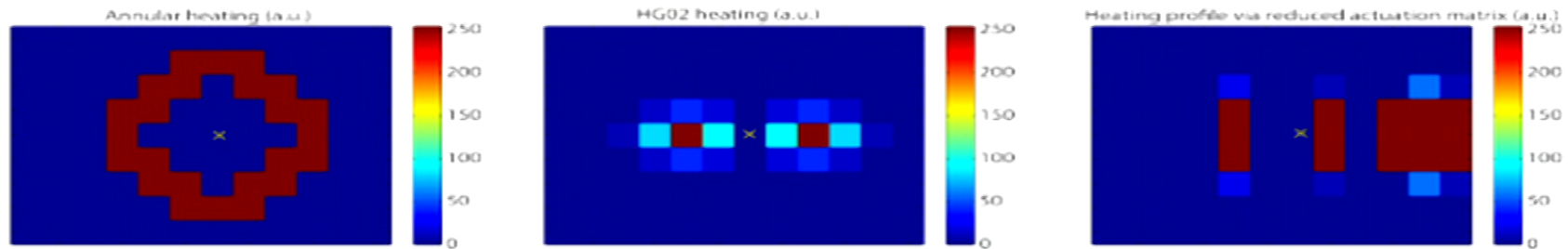




# Heater effect on dark port power



(a) Dark port power.



# Thermorefractive Noise $dn/dT$

- Gets more relevant when lowering the arm Finesse

PHYSICAL REVIEW D **80**, 062004 (2009)

## **Thermorefractive and thermochemical noise in the beamsplitter of the GEO600 gravitational-wave interferometer**

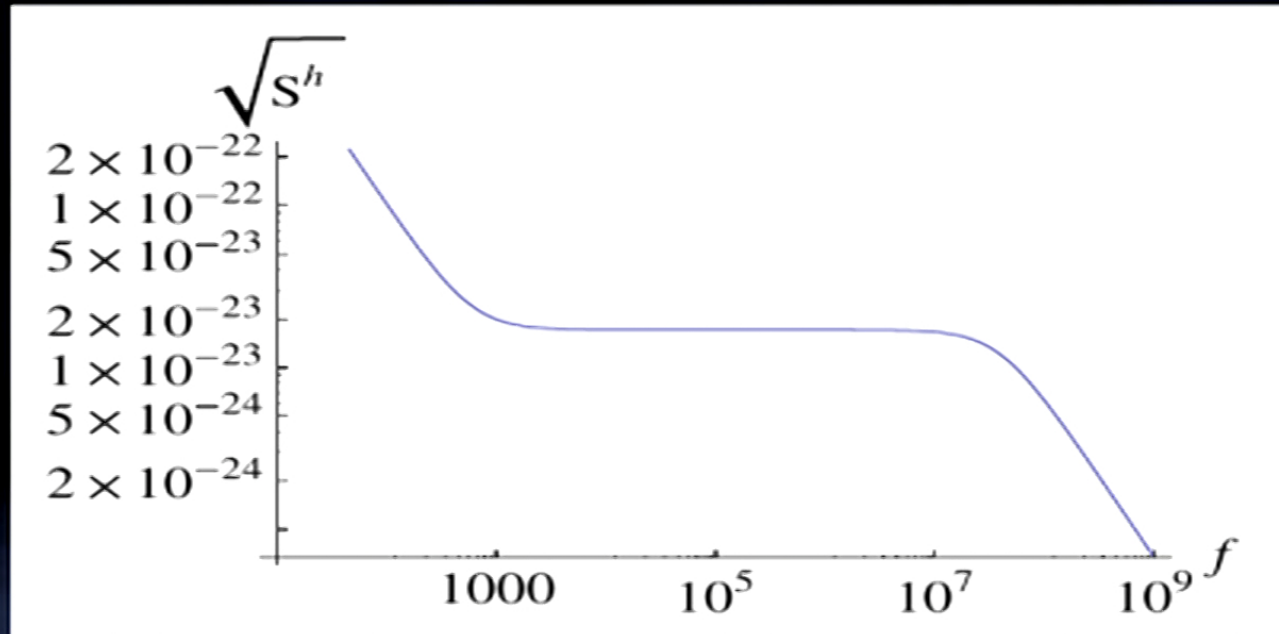
Bruin Benthem and Yuri Levin

*Leiden University, Leiden Observatory and Lorentz Institute, Niels Bohrweg 2, 2300 RA Leiden, the Netherlands*  
(Received 6 July 2009; published 30 September 2009)

Braginsky, Gorodetsky, and Vyatchanin have shown that thermorefractive fluctuations are an important source of noise in interferometric gravitational-wave detectors. In particular, the thermorefractive noise in the GEO600 beamsplitter is expected to make a substantial contribution to the interferometer's total noise budget. Here, we present a new computation of the GEO600 thermorefractive noise, which takes into account the beam's elliptical profile and, more importantly, the fact that the laser beam induces a standing electromagnetic wave in the beamsplitter. The use of updated parameters results in the overall reduction of the calculated noise amplitude by a factor of  $\sim 5$  in the low-frequency part of the GEO600 band, compared to the previous estimates. We also find, by contrast with previous calculations, that thermorefractive fluctuations result in white noise between 600 Hz and 39 MHz, at a level of  $8.5 \cdot 10^{-24} \text{ Hz}^{-1/2}$ . Finally, we describe a new type of thermal noise, which we call the thermochemical noise. This is caused by a random motion of optically active chemical impurities or structural defects in the direction along a steep intensity gradient of the standing wave. We discuss the potential relevance of the thermochemical noise



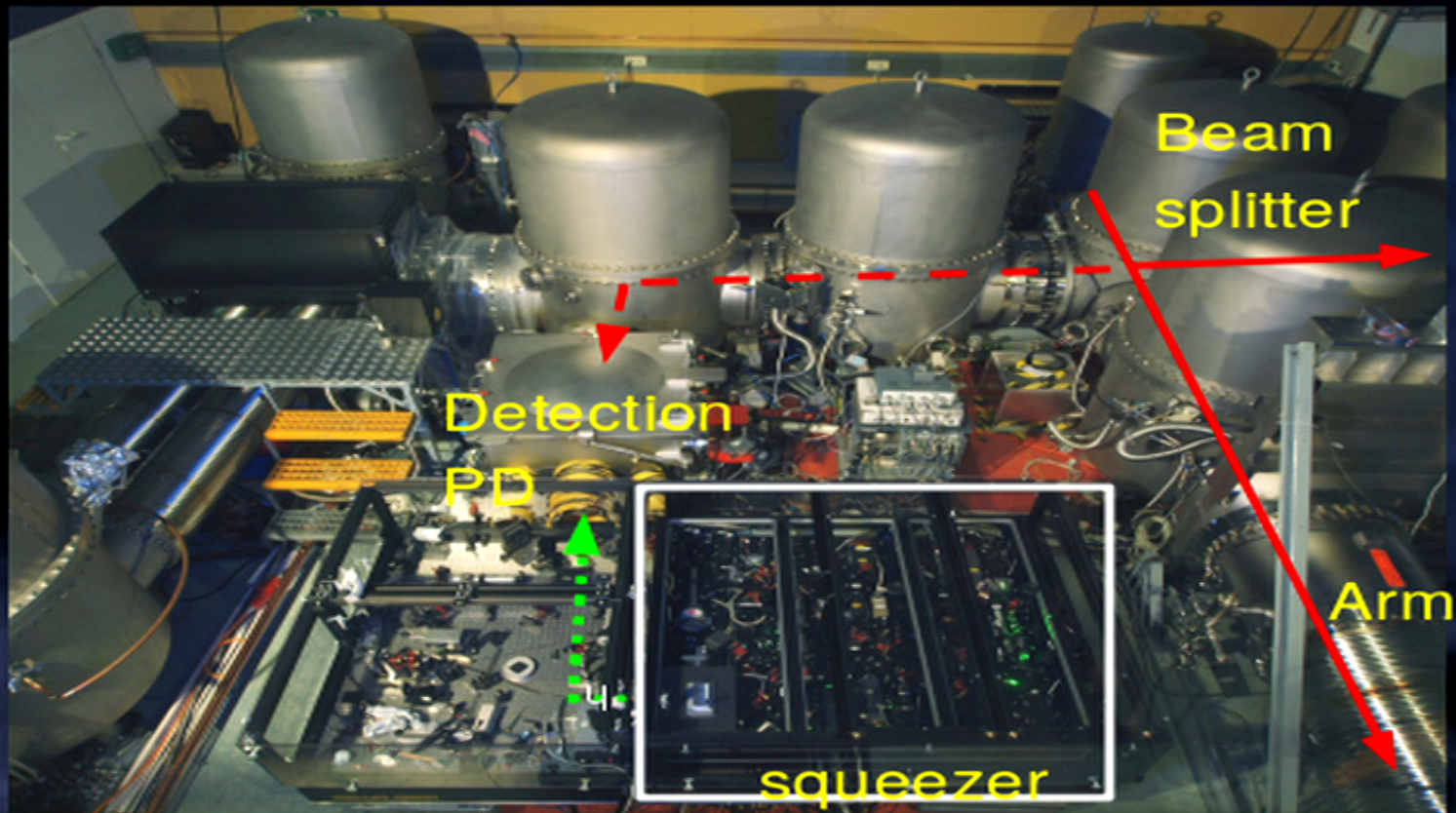
# Thermorefractive Noise for GEO parameters



# (Input) Squeezing



# Input Squeezing at GEO (since 2010)

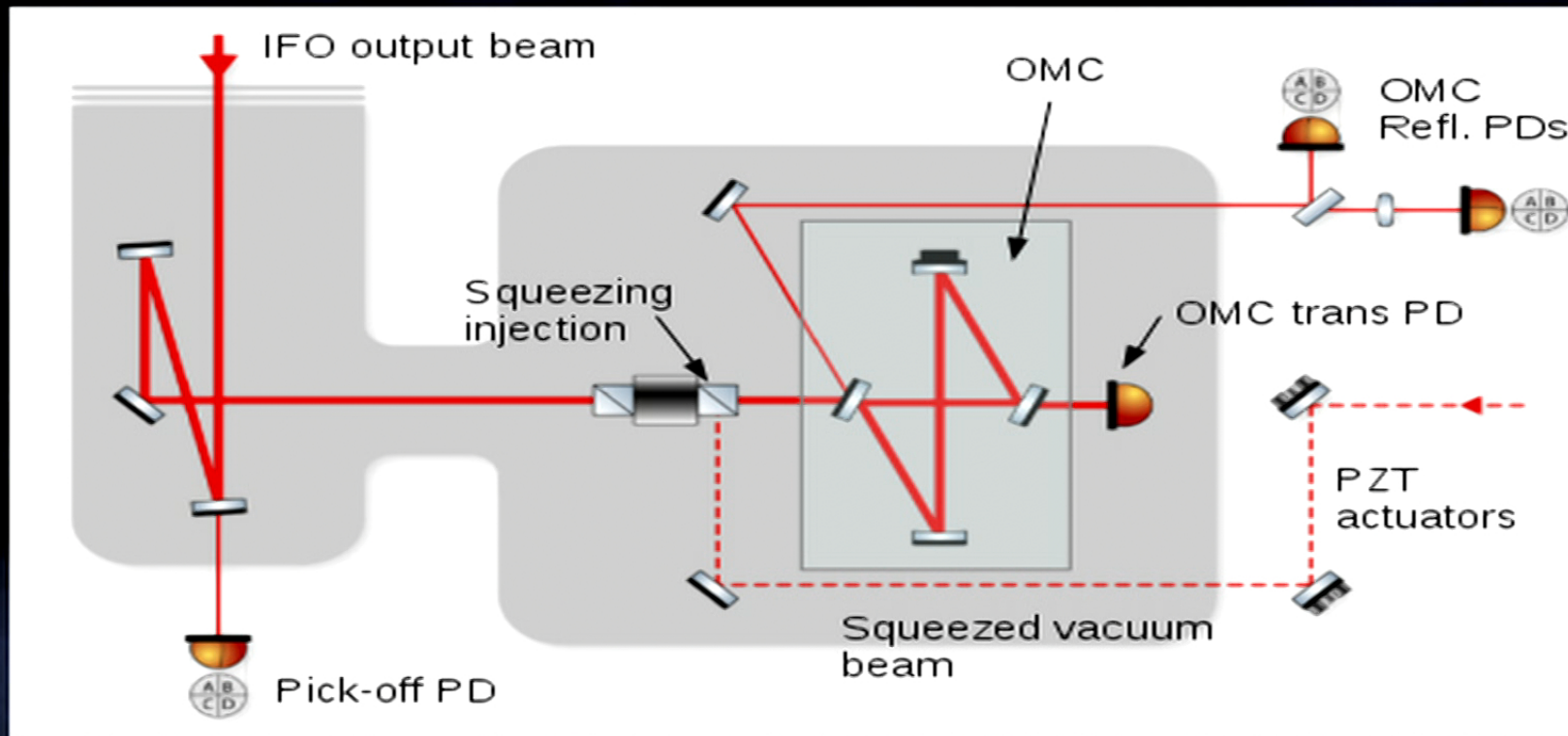


# Squeezing Integration and R&D

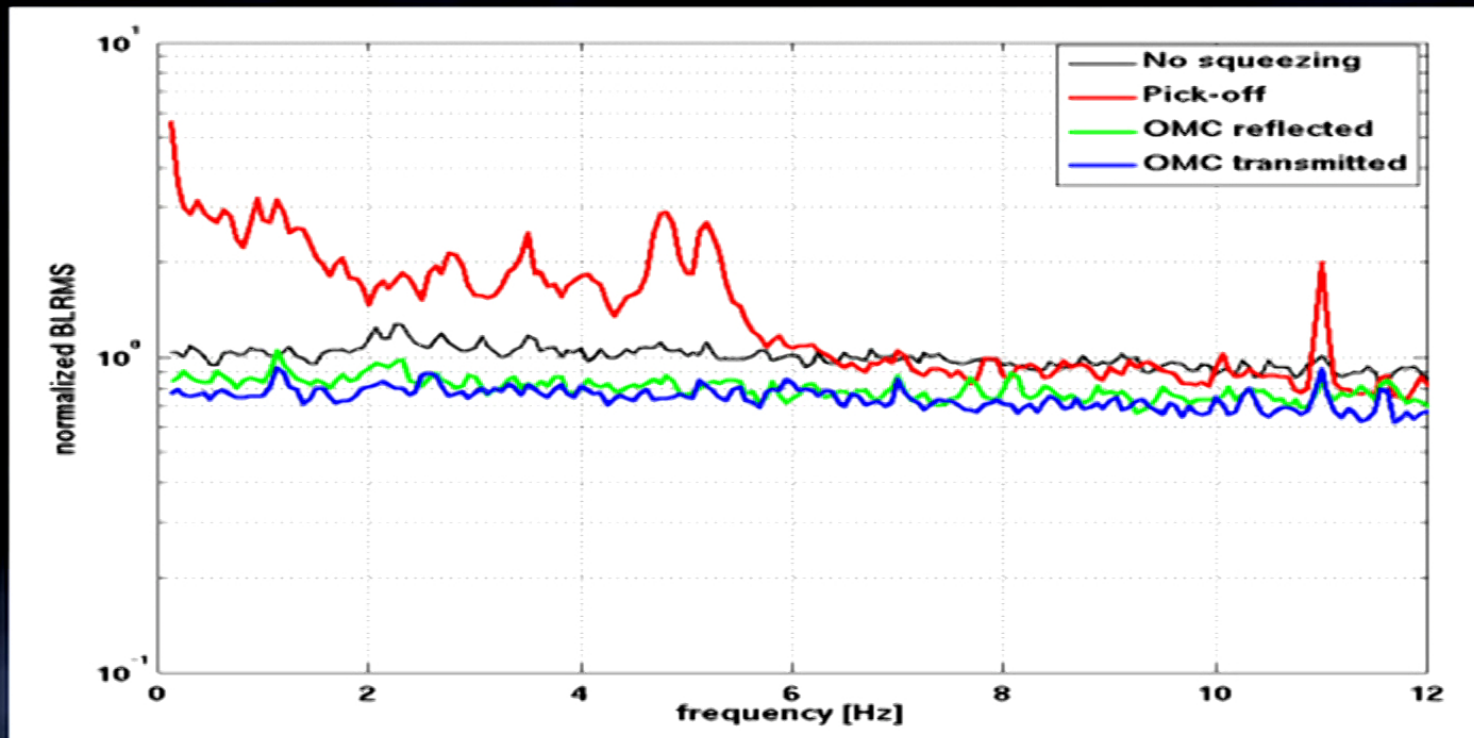
- Long term performance
- Phase control
- Alignment control
- Loss reduction



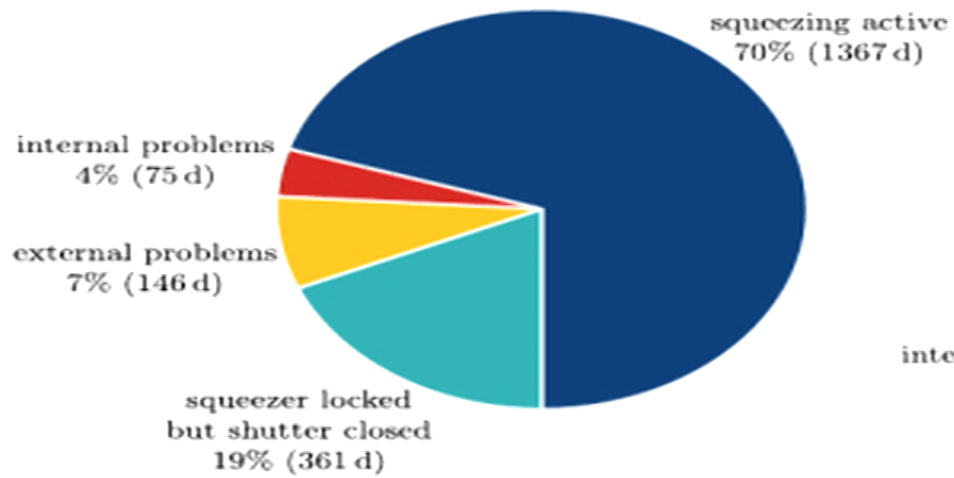
# Squeezing phase and angular control



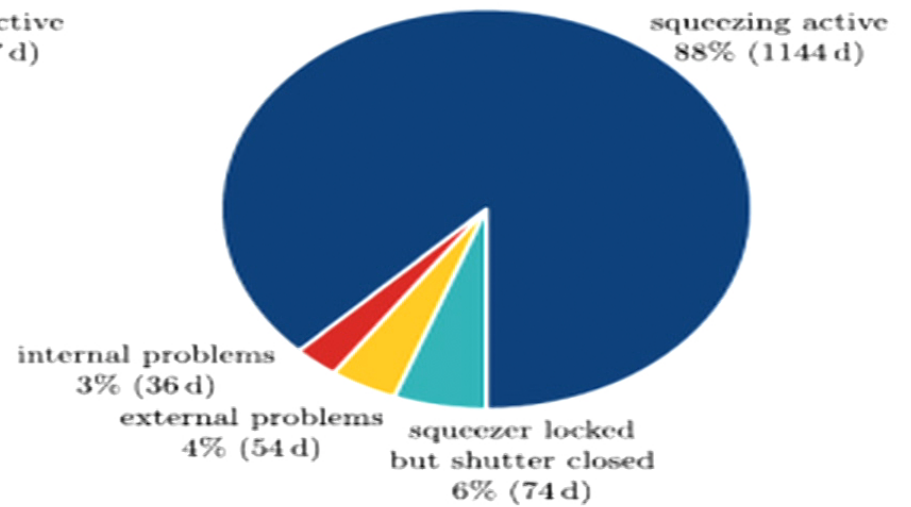
# Fluctuation of squeezed (strain) noise floor for different phase control signals



K. Dooley et al.: P 1400150, Optics Express (2015),  
See also AIC/QNWG session on Tuesday afternoon



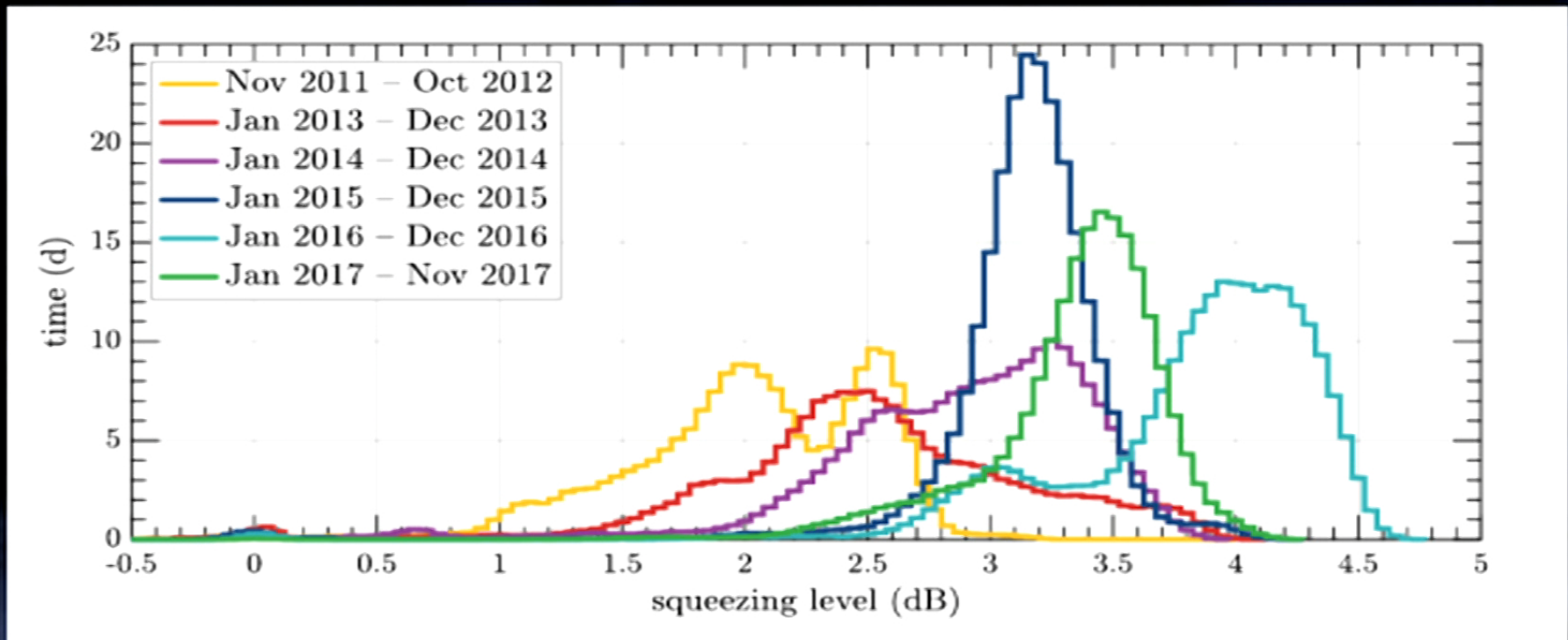
**(a)** Total time (1949 d)

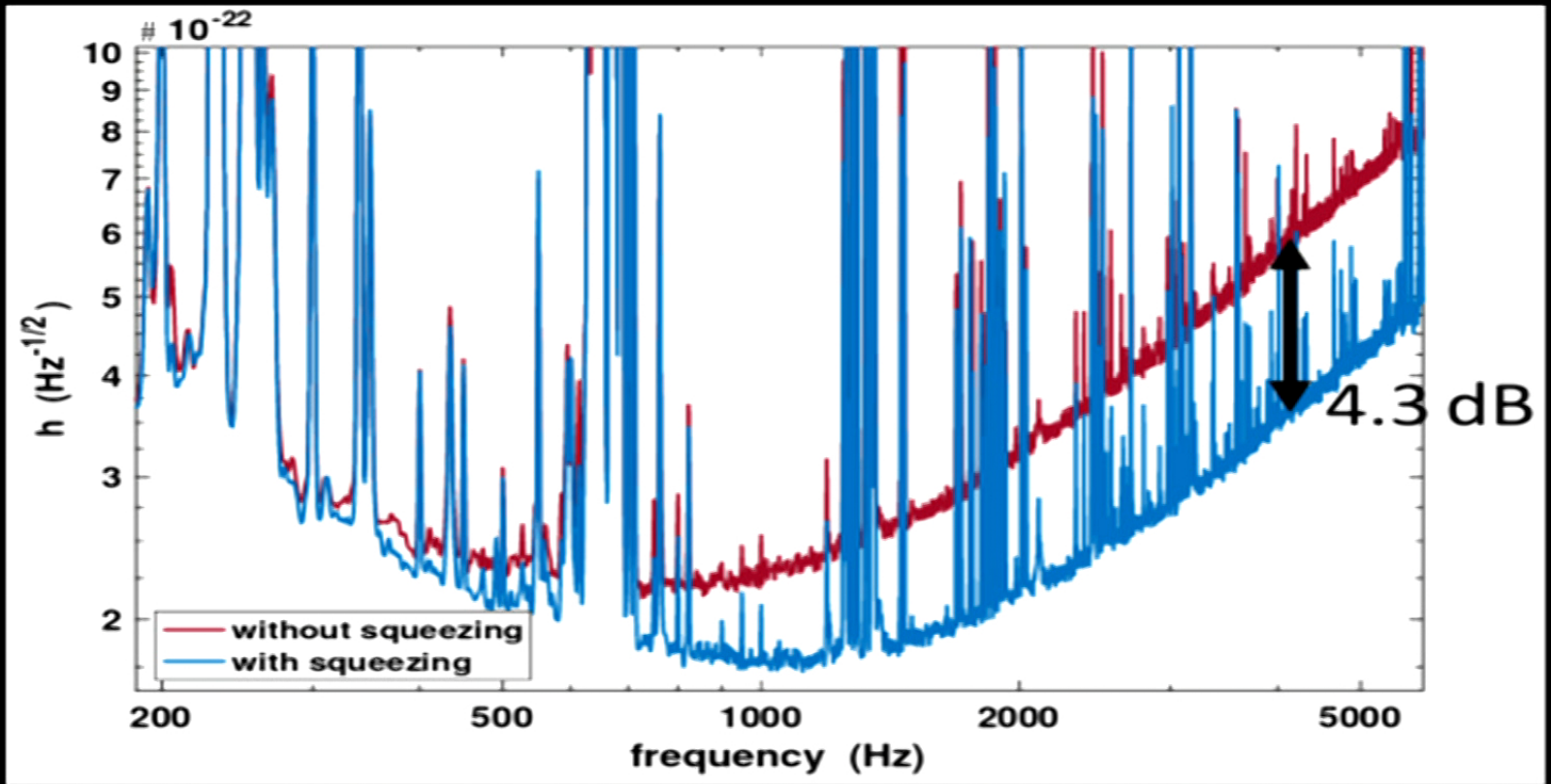


**(b)** Science time only (1306 d)

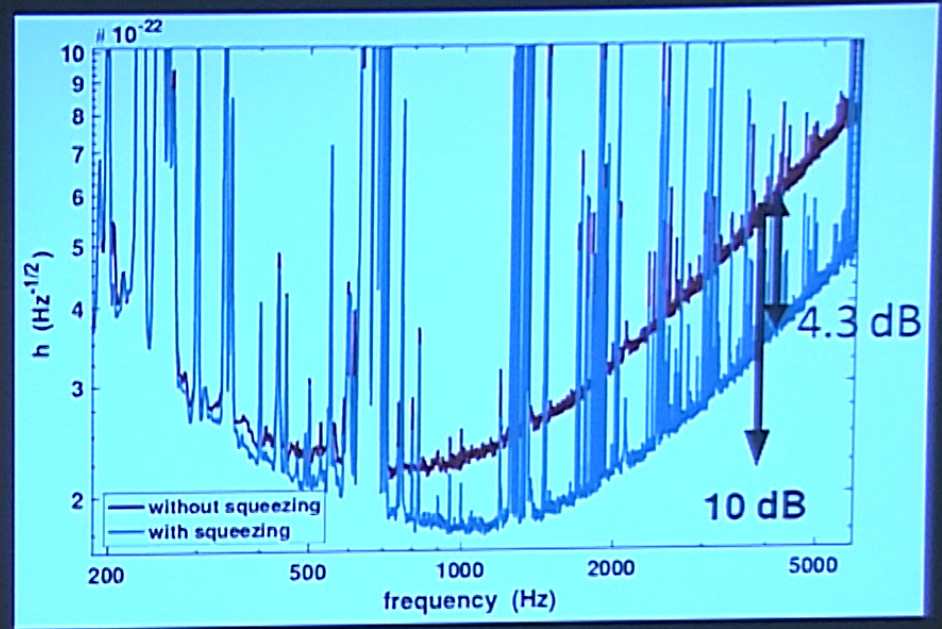
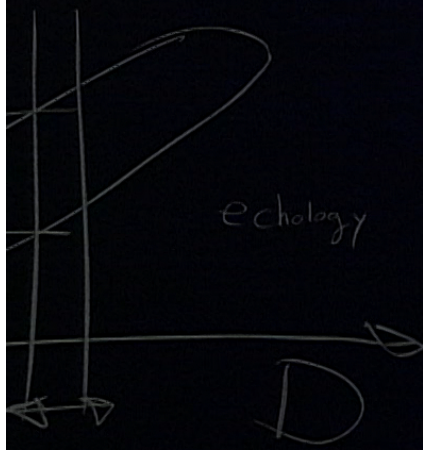


# Long-term performance histograms





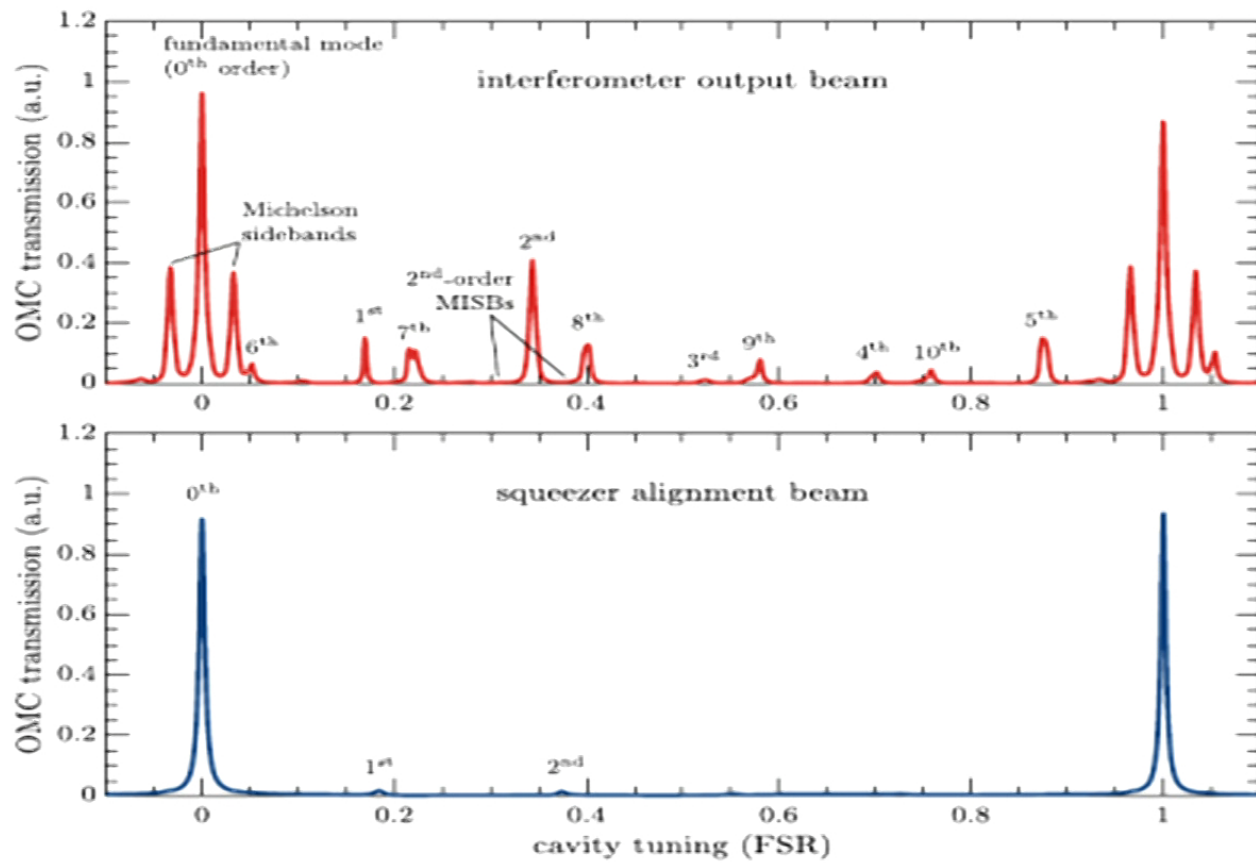
echology



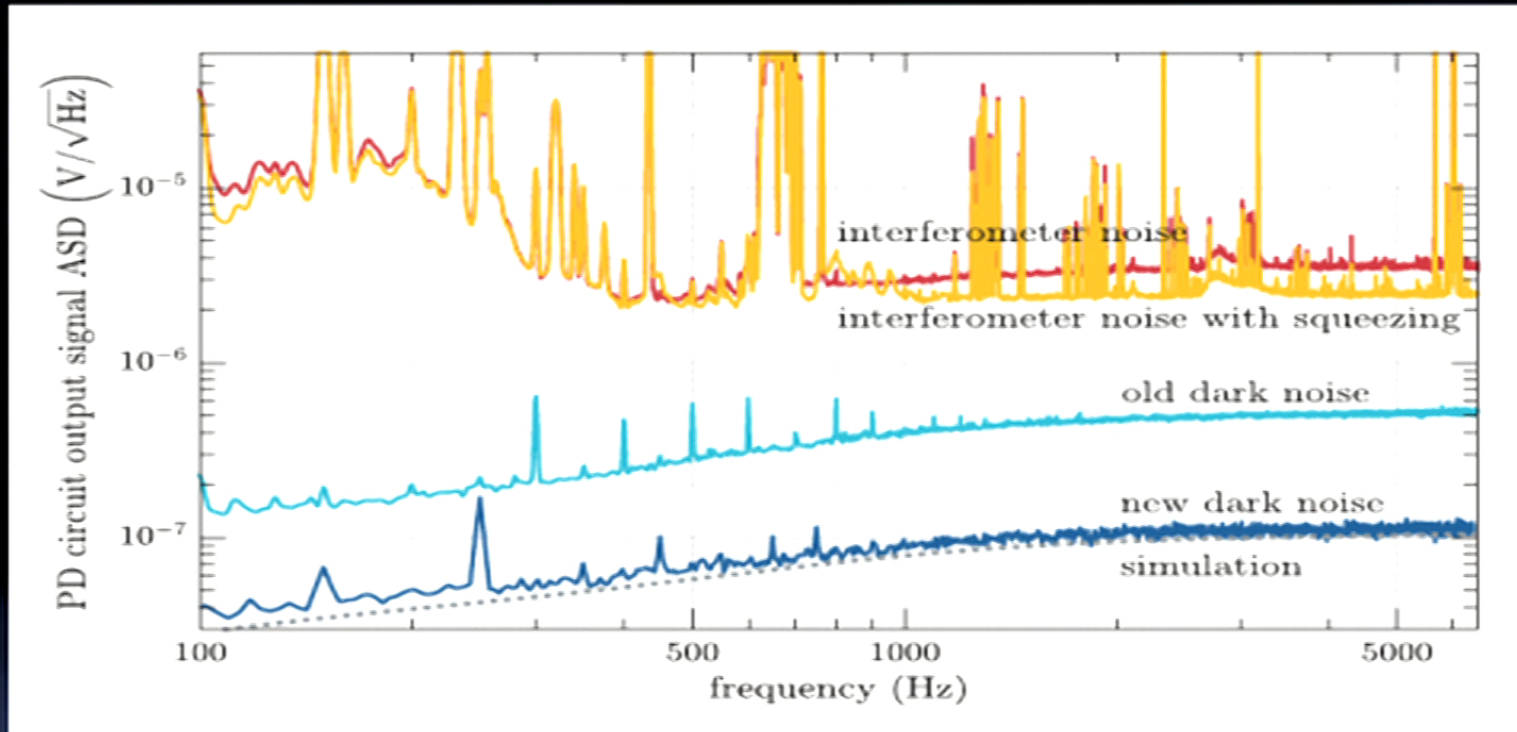
ed lower losses  
optical path and materials



loss mechanism	effective loss (%)
finite OPA escape efficiency	7
lenses, HR mirrors, etc.	3
in-air Faradays (two passes)	$2 \times 3$
injection Faraday (two passes)	$2 \times 4.5$
reflection off interferometer	1
pick off (two passes)	$2 \times 1$
OMC mismatch (all mode orders combined)	5
OMC loss	4
finite PD quantum efficiency	1
total losses	32



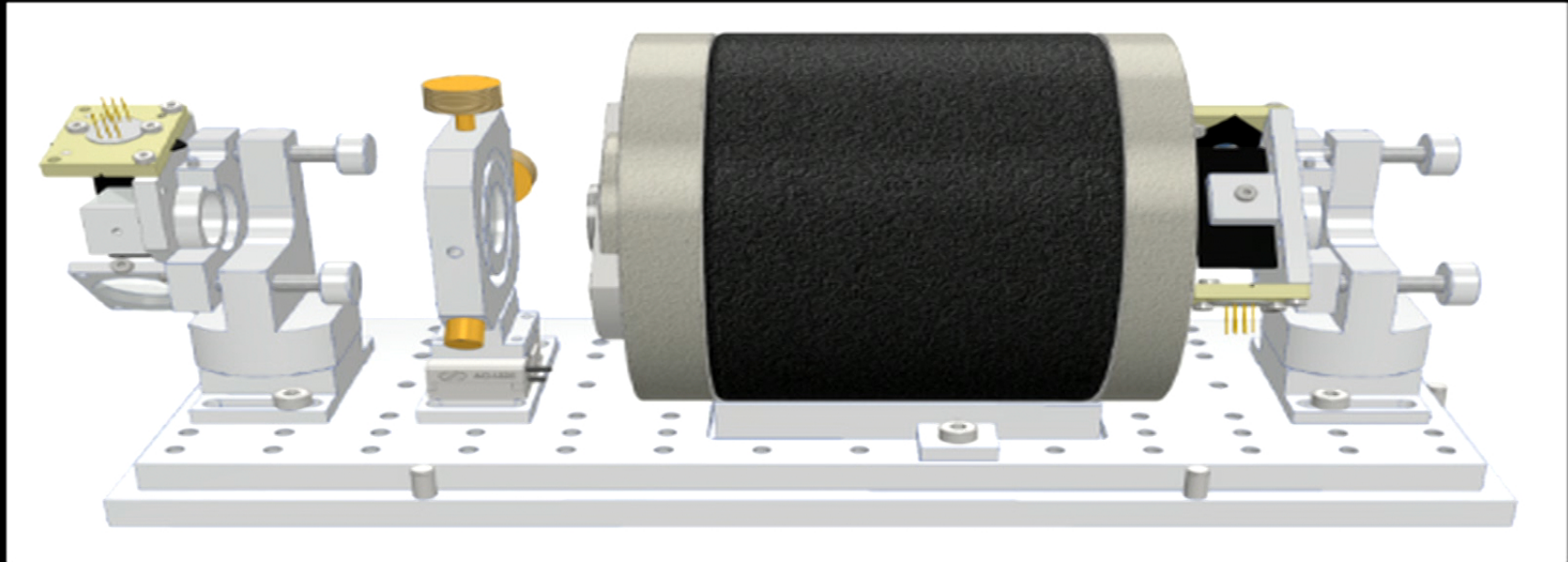
# Increased PD dynamic range by factor 8 with better electronics



0.2dB more squeezing



# More sensing / control of polarization

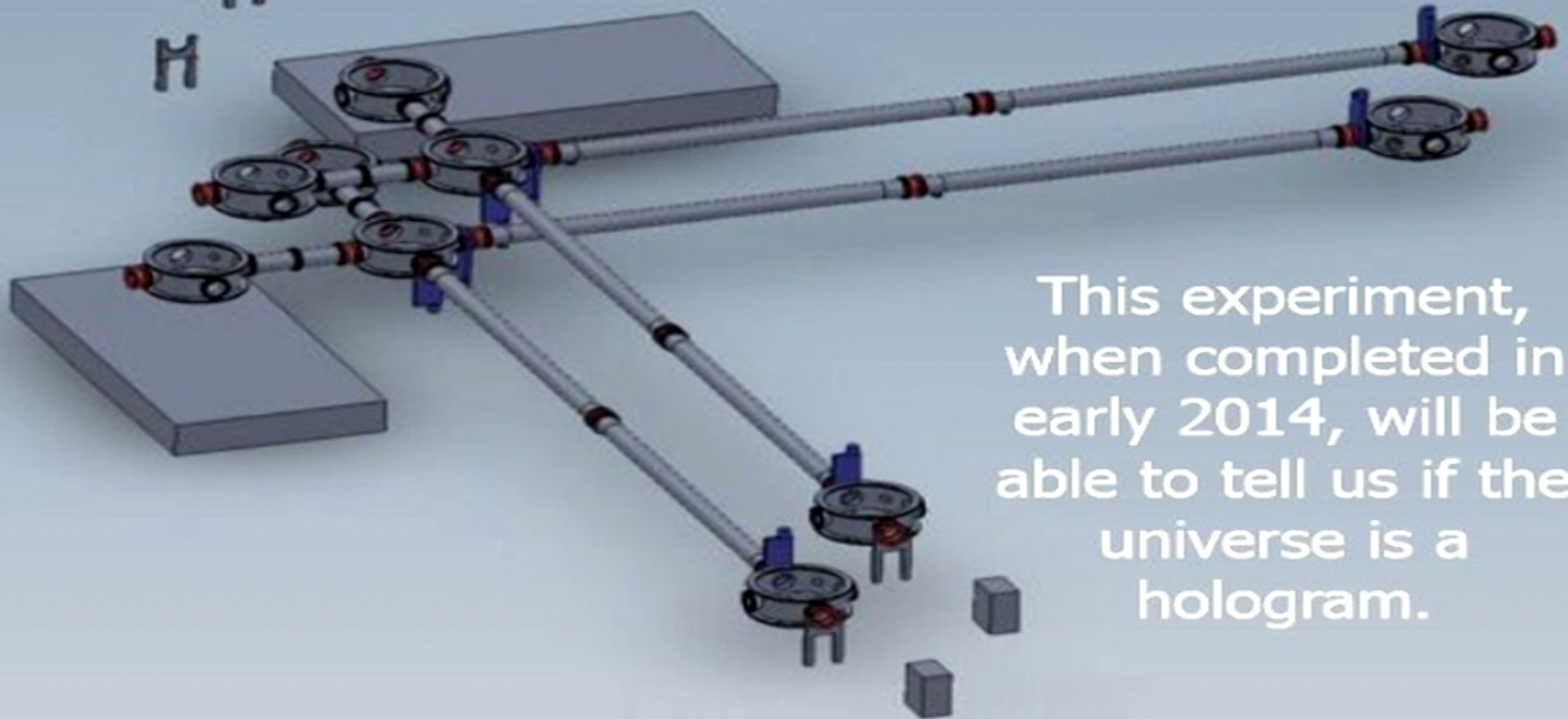


	best so far	in reach	long-term goal
<i>loss mechanisms:</i>			
finite OPA escape efficiency	7%	7%	1%
lenses, HR mirrors, etc.	3%	2%	0.5%
in-air Faradays	2 × 3%	2 × 1%	2 × 0.6%
injection Faraday	2 × 4.5%	2 × 1%	2 × 0.6%
reflection off interferometer	1%	1%	1%
pick off	2 × 1%	2 × 1%	2 × 0.1%
OMC mismatch (all mode orders combined)	5%	3%	1%
OMC loss	4%	4%	1%
finite PD quantum efficiency	1%	1%	0.5%
total losses	32%	22%	7.8%
<i>other imperfections:</i>			
RMS phase noise	20 mrad	15 mrad	10 mrad
dark noise (rel. to unsqz. shot-noise)	0.03	0.03	≤ 0.03
backscattering (rel. to unsqz. shot-noise)	0.01	0.005	≤ 0.003
resulting observed squeezing	4.4 dB	6.2 dB	10.1 dB



# Co-located Interferometers

## Meet Fermilab's Holometer:



This experiment, when completed in early 2014, will be able to tell us if the universe is a hologram.



## Quantum Light in Coupled Interferometers for Quantum Gravity Tests

I. Ruo Berchera,<sup>1</sup> I. P. Degiovanni,<sup>1</sup> S. Olivares,<sup>2</sup> and M. Genovese<sup>1</sup>

<sup>1</sup>*INRIM, Strada delle Cacce 91, I-10135 Torino, Italy*

<sup>2</sup>*Dipartimento di Fisica, Università degli Studi di Milano, and CNISM UdR Milano Statale, Via Celoria 16, I-20133 Milano, Italy*

(Received 22 January 2013; published 21 May 2013)

In recent years quantum correlations have received a lot of attention as a key ingredient in advanced quantum metrology protocols. In this Letter we show that they provide even larger advantages when considering multiple-interferometer setups. In particular, we demonstrate that the use of quantum correlated light beams in coupled interferometers leads to substantial advantages with respect to classical light, up to a noise-free scenario for the ideal lossless case. On the one hand, our results prompt the possibility of testing quantum gravity in experimental configurations affordable in current quantum optics laboratories and strongly improve the precision in “larger size experiments” such as the Fermilab holometer; on the other hand, they pave the way for future applications to high precision measurements and quantum metrology.

DOI: [10.1103/PhysRevLett.110.213601](https://doi.org/10.1103/PhysRevLett.110.213601)

PACS numbers: 42.50.St, 03.65.Ud, 04.60.-m, 42.25.Hz



# Axions

# Axion interferometry

William DeRocco<sup>1</sup> and Anson Hook<sup>1,2</sup>

<sup>1</sup>*Stanford Institute for Theoretical Physics,  
Stanford University, Stanford, CA 94305, USA*

<sup>2</sup>*Maryland Center for Fundamental Physics, Department of Physics  
University of Maryland, College Park, MD 20742.*

We propose using interferometry of circularly polarized light as a mechanism by which to test for axion dark matter. These interferometers differ from standard interferometers only by the addition of a few quarter waveplates to preserve the polarization of light upon reflection. We show that using current technology, interferometers can probe new regions of axion parameter space up to a couple orders of magnitude beyond current constraints.

## I. INTRODUCTION

One of the leading candidates for dark matter (DM) is a light pseudo-scalar derivatively coupled to the Standard Model (SM). The most well-known example of such a candidate is the QCD axion [1, 4]. The axion can have a multitude of different couplings to the SM. The coupling that produces the effect of interest in this article is

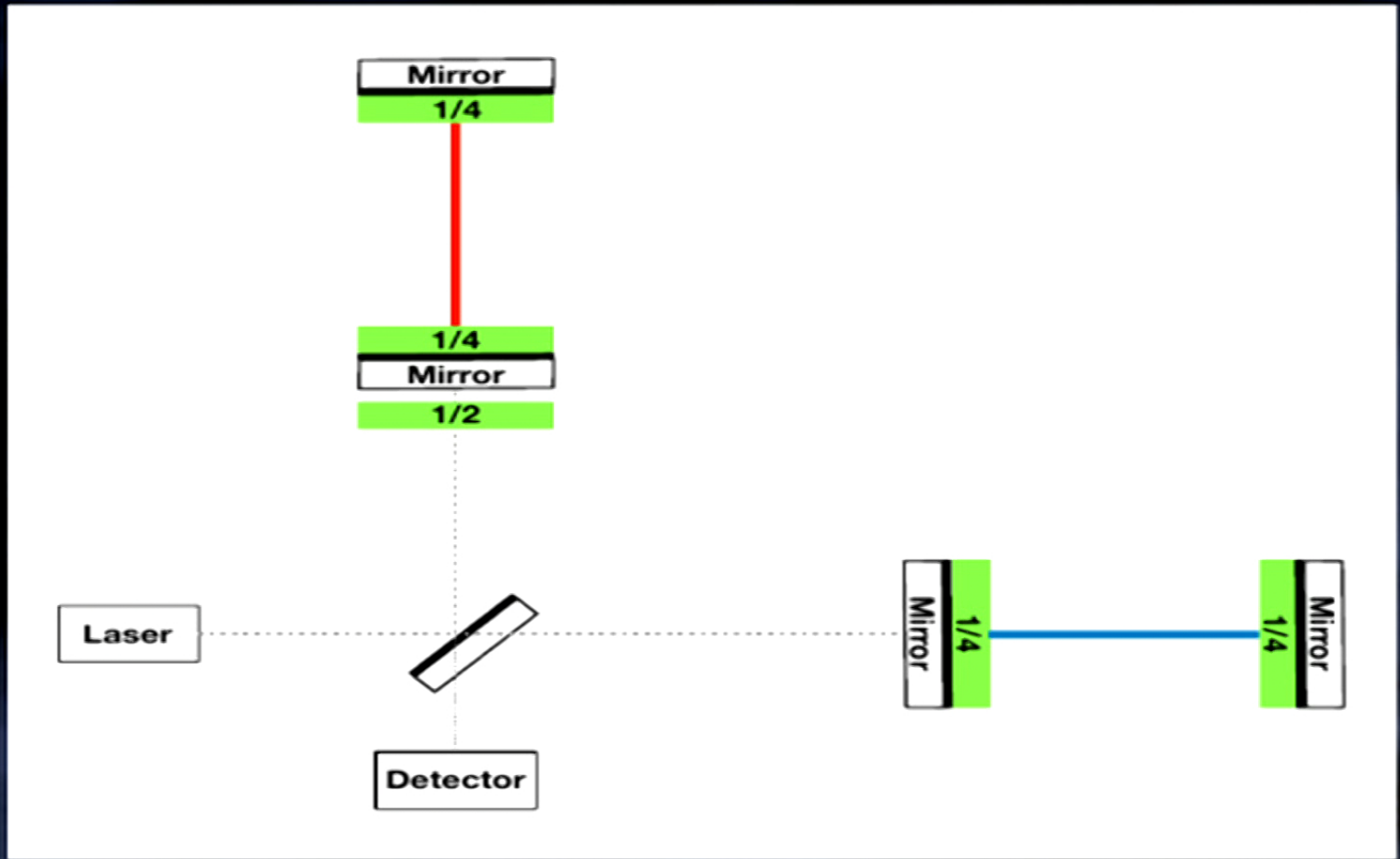
$$\mathcal{L} \supset \frac{a}{4f} F\tilde{F} \quad (1)$$

which is the axion coupling to photons. While in the simplest models of the QCD axion, the axion-photon cou-

## II. MAPPING BETWEEN GRAVITATIONAL WAVES AND AXION DM

If the light in the interferometer is circularly polarized, there is an exact mapping between the effects of axions and gravitational waves. Therefore all of the literature on gravitational wave interferometry can be imported directly into axion interferometry.

To map between gravitational waves and axions, we compare an axion interferometer with left and right polarized light respectively in each of the two arms with a gravitational wave interferometer with arms along the  $x$





RECEIVED: October 16, 2017

REVISED: April 27, 2018

ACCEPTED: June 1, 2018

PUBLISHED: June 7, 2018

## Probing axions with neutron star inspirals and other stellar processes

---

**Anson Hook<sup>a,b</sup> and Junwu Huang<sup>a,c</sup>**

<sup>a</sup> *Stanford Institute for Theoretical Physics, Stanford University,  
Stanford, CA 94305, U.S.A.*

<sup>b</sup> *Maryland Center for Fundamental Physics, University of Maryland,  
College Park, MD 20742, U.S.A.*

<sup>c</sup> *Perimeter Institute for Theoretical Physics,  
Waterloo, Ontario N2L 2Y5, Canada*

*E-mail:* [hook@stanford.edu](mailto:hook@stanford.edu), [jhuang@perimeterinstitute.ca](mailto:jhuang@perimeterinstitute.ca)

# Collision Stop !

Having a new force between neutrons stars is exciting because Advanced LIGO has the potential to detect neutron star mergers and can probe new forces between neutron stars. The fact that the new force has an associated length scale means that at distances  $\sim 1/m_a$ , the frequency of orbit and therefore the frequency of the emitted gravitational waves will change.<sup>3</sup> When the frequency of rotation becomes larger than  $m_a$ , then scalar Larmor radiation can occur and therefore the rate of change of the frequency of the gravitational waves will change. These two physical effects will be the main observable consequence at Advanced LIGO. A more drastic effect occurs when the axion force is stronger than gravity and is repulsive. In this case, the neutron stars do not merge and instead come to rest at a fixed distance apart from each other. The waveform of the gravitational wave emitted in this case has features very different from a merger waveform.

This paper is organized as follows. Section 2 demonstrates that dense objects can source axions, and discusses the analytic calculation of the force between two neutron stars in various limits. Section 3 provides barebones estimates of how a new force between neutron stars would manifest itself at Advanced LIGO. Section 4 supplies some constraints on these models coming from other processes. Finally, we conclude in section 5.